Proc. Natl. Acad. Sci. USA
Vol. 93, pp. 2511–2516, March 1996
Biochemistry

Large electrostatic differences in the binding thermodynamics of a cationic peptide to oligomeric and polymeric DNA

WENTAO ZHANG*, JEFFREY P. BOND*, CHARLES F. ANDERSON*, TIMOTHY M. LOHMAN†, AND M. THOMAS RECORD, JR.*‡§

Departments of *Chemistry and ‡Biochemistry, University of Wisconsin, Madison, WI 53706; and †Department of Biochemistry and Molecular Biophysics, Washington University School of Medicine, St. Louis, MO 63110

Communicated by Peter H. von Hippel, University of Oregon, Eugene, OR, December 15, 1995 (received for review October 24, 1995)

ABSTRACT **Results presented here demonstrate that the thermodynamics of oligocation binding to polymeric and oligomeric DNA are not equivalent because of long-range electrostatic effects. At physiological cation concentrations (0.1–0.3 M) the binding of an oligolysine octacation KWK_6-NH_2 (+8 charge) to single-stranded poly(dT) is much stronger per site and significantly more salt concentration dependent than the binding of the same ligand to an oligonucleotide, $dT(pdT)_{10}$ (−10 charge). These large differences are consistent with Poisson–Boltzmann calculations for a model that characterizes the charge distributions with key preaveraged structural parameters. Therefore, both the experimental and the theoretical results presented here show that the polyelectrolyte character of a polymeric nucleic acid makes a large contribution to both the magnitude and the salt concentration dependence of its binding interactions with simple oligocationic ligands.**

All crystallographic and NMR structure determinations and numerous experimental and theoretical studies of the binding of cationic ligands and proteins to DNA in solution have been performed with oligo(deoxy)nucleotides. Use of oligonucleotides in solution studies provides an efficient means of examining effects of changes in sequence and is the only means of eliminating effects of cooperativity due to protein–protein interactions on a longer DNA lattice (1, 2). Results of thermodynamic and kinetic studies of ligand–oligonucleotide interactions, and the corresponding theoretical analyses based on structures of oligonucleotide complexes, pertain directly to polymeric DNA only if interactions involving regions that flank the binding site are negligible (or can be taken properly into account). For example, short oligonucleotides are oligoelectrolytes, which differ strikingly in their interactions with salt ions from the behavior of polyelectrolytes. The polyelectrolyte character of polymeric DNA has been proposed (3, 4) as the primary origin of the large dependences on salt concentration observed for the binding both of simple oligocations (5–7) and of locally cationic surface regions of proteins (3, 4) to polymeric DNA. At low salt concentrations ($\lesssim$10 mM), this "polyelectrolyte effect" has a sound theoretical basis (3, 4, 8). At higher salt concentrations, however, some more recent theoretical developments (9–12) have raised questions about the importance of the polyelectrolyte character of DNA as a determinant of its thermodynamic activity and hence of its ligand-binding energetics. To address this controversy, we report here the first direct experimental comparison of the magnitudes and salt concentration dependences of nonspecific binding affinities of a peptide cationic ligand (KWK_6-NH_2) to two lengths of DNA: one [poly(dT)] long enough so that virtually all potential binding sites are in the interior of the polyion and the other [$dT(pdT)_{10}$] so short that it has no polyelectrolyte character.

The effective range of electrostatic interactions between charges in solution determines not only the number of nucleic acid phosphates that contribute to the polyelectrolyte effect but also the number of parameters needed to describe this effect theoretically. A recent review (13) of electrostatic calculations on biomolecules has stressed the importance of modeling the interacting species with all available structural detail. This approach may be appropriate for systems and/or conditions where the governing interactions are predominantly short range and where this level of structural detail is uniformly available for all participants. However, for nucleic acids and their complexes complete structural details in solution are rarely available. Fortunately, a considerable body of evidence (reviewed in ref. 14) indicates that under typical experimental conditions (including physiological salt concentrations) the effective range of electrostatic interactions is long enough so that many pairwise interactions contribute to the electrostatic potential acting on the surface of DNA. Consequently, specification of the precise location of each charge is anticipated to be relatively less significant. Therefore, a small number of preaveraged structural parameters may suffice to describe the important characteristics of the charge distributions that determine salt concentration effects on equilibria such as oligocation binding to a nucleic acid. To determine whether mean axial charge densities and hard core distances of closest approach suffice to characterize thermodynamic effects of the interactions of salt ions with KWK_6-NH_2, poly(dT) and $dT(pdT)_{10}$, effects of varying the salt concentration on the binding of this octacation to both lengths of DNA were calculated using the cylindrical Poisson–Boltzmann (PB) equation (14).

MATERIALS AND METHODS

Buffers. All chemicals were reagent grade and solutions were prepared with distilled-deionized Milli-Q H_2O (Millipore). All experiments were performed in 5 mM sodium cacodylate/0.2 mM Na_3EDTA buffer, pH 6.0, at 25°C with variable amounts of sodium acetate (NaOAc).

Nucleic Acids. Poly(dT) (average length of 3000 phosphate charges) was purchased from Sigma and dialyzed extensively to remove excess salt. The oligonucleotide $dT(pdT)_{10}$ was obtained from Operon Technologies (Alameda, CA) and purified using a Hamilton PRP-1 reverse-phase HPLC column in volatile salt (triethylamine acetate) buffer. The excess salt was removed by evaporation. Concentrations of poly(dT) and $dT(pdT)_{10}$ were determined spectrophotometrically at 260 nm using $\varepsilon_{260} = 8100\ M^{-1}\cdot cm^{-1}$ (6, 15).

The publication costs of this article were defrayed in part by page charge payment. This article must therefore be hereby marked "*advertisement*" in accordance with 18 U.S.C. §1734 solely to indicate this fact.

Abbreviations: PB, Poisson–Boltzmann; GCMC, grand canonical Monte Carlo.

§To whom reprint requests should be addressed at: Department of Biochemistry, 420 Henry Mall, University of Wisconsin, Madison, WI 53706.

Oligopeptide. KWK_6-NH_2 (K, L-lysine; W, L-tryptophan), a tryptophan-containing oligolysine amide, was synthesized by the Fmoc (fluorenyl-9-methoxycarbonyl) solid-phase method using the procedure described by Houghten *et al.* (16). The crude peptide was then purified on a Kromasil (Eka Nobel, Sweden) 100A 5-μm C_{18} reverse-phase column using water/acetonitrile (0.1% trifluoroacetic acid) gradients to yield ≈99% pure peptide. Peptide identity was confirmed by mass spectrometry. Tryptophan was incorporated near the N terminus of the peptide to permit fluorescence measurements of binding and determinations of peptide concentrations from the absorbance at 280 nm in 6 M guanidium hydrochloride using $\varepsilon_{280} = 5690\ M^{-1}\cdot cm^{-1}$ (17).

Fluorescence Measurements. Tryptophan fluorescence was monitored to quantify the binding of KWK_6-NH_2 to single-stranded poly(dT) and to dT(pdT)$_{10}$ at an excitation wavelength of 296 nm and an emission wavelength of 350 nm (18) using an SLM Aminco (Urbana, IL) model 8000C spectrofluorometer. The observed fluorescence quenching, Q_{obs}, is defined as $Q_{obs} \equiv (F_o - F_{obs})/F_o$ where F_o is the initial fluorescence of the free peptide and F_{obs} is the observed fluorescence during titrations. Small corrections of Q_{obs} for dilution, the inner filter effect, photobleaching, as well as background emission and Raman light scattering from water, were applied to obtain the corrected fluorescence quenching, Q_{corr} (18, 19). Q_{corr} was directly proportional to $[L_B]/[L_T]$ using binding density function analysis (18), where $[L_B]$ and $[L_T]$ are the concentrations of bound and total peptide, respectively. Thus, the binding density, ν, expressed as the average fraction of a ligand bound per site and the free ligand concentration, $[L_F]$, can be calculated from fluorescence quenching data using $\nu = (Q_{corr}/Q_{max})([L_T]/[D_T])$ and $[L_F] = (1 - Q_{corr}/Q_{max})[L_T]$, respectively, where $[D_T]$ is the total concentration of DNA sites. The maximum fluorescence quenching, Q_{max}, was determined by a linear extrapolation of Q_{corr} to $[L_B]/[L_T] = 1$.

Binding Isotherms. "Reverse" titrations, where the peptide is titrated with DNA, were used to construct binding isotherms (18). Binding of KWK_6-NH_2 (L^{8+}) to DNA is represented as the binding of a free ligand, L_F, to an isolated free DNA site, S_F (a site is considered to be 8 consecutive phosphates for KWK_6-NH_2), to form complex C, according to the stoichiometry: $L_F + S_F \rightleftarrows C$. We assume that the number of available binding sites on a totally uncomplexed dT N-mer (with N phosphates) is $N - 8 + 1$ (20). Thus, on poly(dT) ($N \approx 3 \times 10^3$), the potential number of binding sites is approximately N; on dT(pdT)$_{10}$ ($N = 10$), there are three potential overlapping binding sites, all of which are eliminated by binding one ligand. The equilibrium constant, K_{obs}, for binding of KWK_6-NH_2 to poly(dT) is obtained from the standard McGhee–von Hippel isotherm (20)

$$K_{obs} = \frac{1}{[L_F]}\frac{\nu}{1-n\nu}\left(\frac{1-(n-1)\nu}{1-n\nu}\right)^{n-1}, \qquad [1]$$

derived from a noncooperative neighbor exclusion model for a one-dimensional infinite homogeneous lattice. For dT-(pdT)$_{10}$, binding one ligand at any of the three available sites on the oligomer saturates its binding capacity. Thus, for binding to dT(pdT)$_{10}$, Eq. **1** reduces to

$$K_{obs} = \frac{1}{[L_F]}\frac{\nu}{1-n\nu}, \qquad [2]$$

with $n = 3$. In both Eqs. **1** and **2**, n is the overlap-site size—i.e., the number of binding sites occluded by the bound ligand [$n = 8$ for binding to poly(dT) and $n = 3$ for binding to dT(pdT)$_{10}$]. Nonlinear least-squares fittings to the fluorescence quenching data based on Eqs. **1** and **2** were performed to obtain K_{obs} for KWK_6-NH_2 binding to poly(dT) and to dT(pdT)$_{10}$, respectively.

Salt Concentration Dependence of K_{obs}. "Salt-back" titrations (18), where preformed peptide–DNA complexes are dissociated by titration with concentrated NaOAc solution, were used to obtain K_{obs} at different salt concentrations. Since Q_{max} and n are independent of salt concentration, and $Q_{corr}/Q_{max} = [L_B]/[L_T]$ holds for the salt concentration range studied (7), Eqs. **1** and **2** were used to calculate K_{obs} in salt-back titrations. To avoid possible aggregation and complications of analyzing data obtained at high binding density (6, 18), the ligand binding density did not exceed 30% of the maximum ($\nu_{max} = 1/n$) in the salt-back titrations of the KWK_6-NH_2/poly(dT) mixture. The effect of uniunivalent salt concentration (expressed by the mean ionic activity $a_\pm$) on a binding equilibrium (designated as S_aK_{obs}) was determined from the tangent line of the weighted quadratic fitting of the $\log K_{obs} - \log a_\pm$ plot. Tabulated experimental values of the molal activity coefficients and densities of NaOAc solutions (21) were used to convert salt concentrations to $a_\pm$ by assuming that the nonideality of the buffer anion is the same as that of OAc^-, which is the dominant anion contributing at least 95% of the total anion concentrations in all experiments.

PB Calculations of S_aK_{obs}. A general thermodynamic analysis (8, 22) of the effect of excess uniunivalent salt on a binding equilibrium yields the following expression:

$$S_aK_{obs} \equiv \frac{d\log K_{obs}}{d\log a_\pm} = (|Z_C| + 2\Gamma_C) - (|Z_D| + 2\Gamma_D) - (|Z_L| + 2\Gamma_L), \qquad [3]$$

where the subscripts C, L, and D indicate complex, ligand, and uncomplexed DNA species, respectively. In Eq. **3**, the net number of charges on each species is Z_J (J = C, L, or D), and Γ_J is the preferential interaction coefficient that characterizes the interactions of excess uniunivalent salt with the corresponding electroneutral component (22). Values of S_aK_{obs} were calculated by using the cylindrical PB equation to evaluate preferential interaction coefficients in Eq. **3** for preaveraged structural models of the octacationic ligand (L^{8+}), the oligomeric or polymeric nucleic acid, and their complex. A finite difference form of the nonlinear PB equation in cylindrical coordinates (the electrostatic potential varies with the cylindrical r and z but not the Θ coordinate) was solved on a nonuniform grid using Gauss–Seidel iteration (23). Increases in the cell size or the density of grid points did not alter the results. Specific details will be published elsewhere. For the uncomplexed DNA and unbound L^{8+} the "standard" (**b**/ε/**a**) model was assumed (cf. ref. 14 for a review); where **b** is the average spacing between structural charges projected onto the axis of a rod-like oligo- or polyion, **a** is the distance of closest approach of the center of a mobile ion to the axis of the nucleic acid or ligand, and $\varepsilon = 78.7$ is the dielectric constant of water at 25°C. Structural parameters of the single stranded DNA (**b** = 3.45 Å, **a** = 10 Å) were those used by Olmsted *et al.* (24) and structural parameters of the model ligand L^{8+} (**b** = 1.7 Å, **a** = 13 Å) were taken from Olmsted *et al.* (8). Neither was optimized for the present analysis. Oligomer termini were modeled as described (8). To model the DNA–L^{8+} complex, a segment of the axial charge on the model DNA containing 8 consecutive charges was eliminated. For dT(pdT)$_{10}$ this segment was in the central position. The radial distance of closest approach of ions to the DNA–L^{8+} complex axis was 14.6 Å over a distance of 36.2 Å centered at the L^{8+} binding site (so that there was no change in the volume excluded to ions upon complexation).

RESULTS

Characterization of L^{8+}–DNA Binding. Reverse titrations performed at constant salt concentration [0.1 M for dT(pdT)$_{10}$

and 0.2 M for poly(dT)] were analyzed to obtain the binding isotherms in Fig. 1. Similar modes of peptide binding are indicated by the identical Q_{max} values (0.90 ± 0.02) observed for both lengths of DNA, as shown in Fig. 1 (*Inset*). The linear plot of Q_{corr} versus $[L_B]/[L_T]$ demonstrates that Q_{corr} is directly proportional to $[L_B]/[L_T]$ over the entire range of binding densities. The stoichiometry of binding was estimated by performing reverse titrations at high binding affinity conditions (6.4 mM Na^+) where distinct stoichiometric end points were observed (shown in Fig. 2). As expected for an oligocationic ligand with 8 positive charges, the stoichiometry for KWK_6-NH_2 binding to poly(dT) is one ligand bound per 8 DNA phosphates (shown in Fig. 2*B*), which is in excellent agreement with that obtained from binding density function analysis (6, 7). Fig. 2*B* indicates that KWK_6-NH_2 forms a 1:1 complex with $dT(pdT)_{10}$. The observations that KWK_6-NH_2 forms a 1:1 complex with $dT(pdT)_{10}$ and occupies 8 phosphates on poly(dT) indicate that there are no putative complexes in which the ligand overhangs the end of $dT(pdT)_{10}$. Fig. 1*B* shows the theoretical isotherm for binding to poly(dT) generated using Eq. **1** with $n = 8$, $Q_{max} = 0.90$ and $K_{obs} = 5.4 \times 10^4\ M^{-1}$. As shown in Fig. 1*B*, the noncooperative form of the McGhee–von Hippel equation (cf. Eq. **1**) successfully describes the effects on the experimental binding isotherm due to the reduction in available binding sites as a function of ligand binding density. Fig. 1*A* shows the theoretical isotherm for binding to $dT(pdT)_{10}$ generated using Eq. **2** with $n = 3$, $Q_{max} = 0.90$, and $K_{obs} = 4.6 \times 10^4\ M^{-1}$. An analysis consistent with the McGhee–von Hippel equation (cf. Eq. **2**) accounts for the observation that binding one ligand effectively saturates the binding capacity of $dT(pdT)_{10}$.

Large Differences in K_{obs} for L^{8+} Binding to Poly(dT) and to $dT(pdT)_{10}$ at Low Salt Concentration. For KWK_6-NH_2 binding to DNA, K_{obs} was determined as a function of salt concentration systematically from 0.1 to 0.5 M salt using salt-back titrations. Typical salt-back titration curves and resultant values of K_{obs} as a function of salt concentration are shown in Fig. 3. More than 95% of the original signal was recovered at the high salt concentrations for both poly(dT) and $dT(pdT)_{10}$, indicating that most of the ligand–DNA complexes were dissociated as the salt concentration increased. Values of K_{obs} for binding to $dT(pdT)_{10}$ and to poly(dT) are similar at high salt concentration (>0.3 M). K_{obs} is $\approx 10^3\ M^{-1}$ for binding L^{8+} to $dT(pdT)_{10}$ and to poly(dT) at 0.3 M salt. For both lengths of DNA, K_{obs} increases with decreasing salt concen-

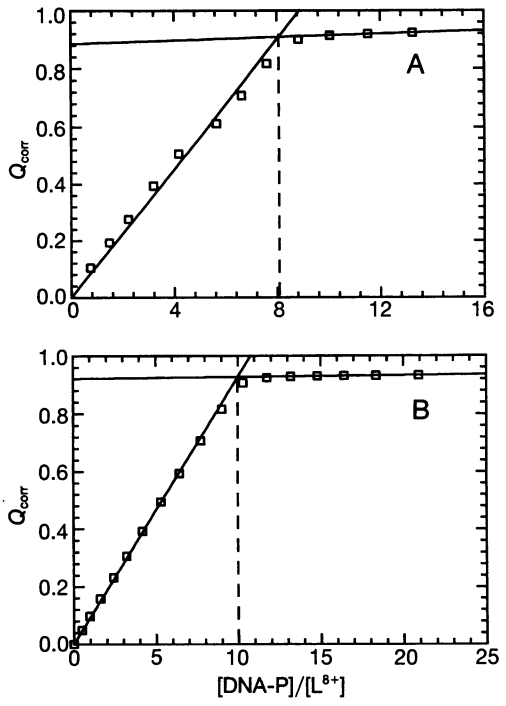

FIG. 2. Reverse titrations represented by Q_{corr} as a function of the ratio of DNA phosphate concentration to ligand concentration ([DNA-P]/[L^{8+}]) as a way to estimate the stoichiometry for KWK_6-NH_2 binding to poly(dT) (*A*) and to $dT(pdT)_{10}$ (*B*). Stoichiometric end points estimated by crossing points of the solid lines are indicated by dashed lines.

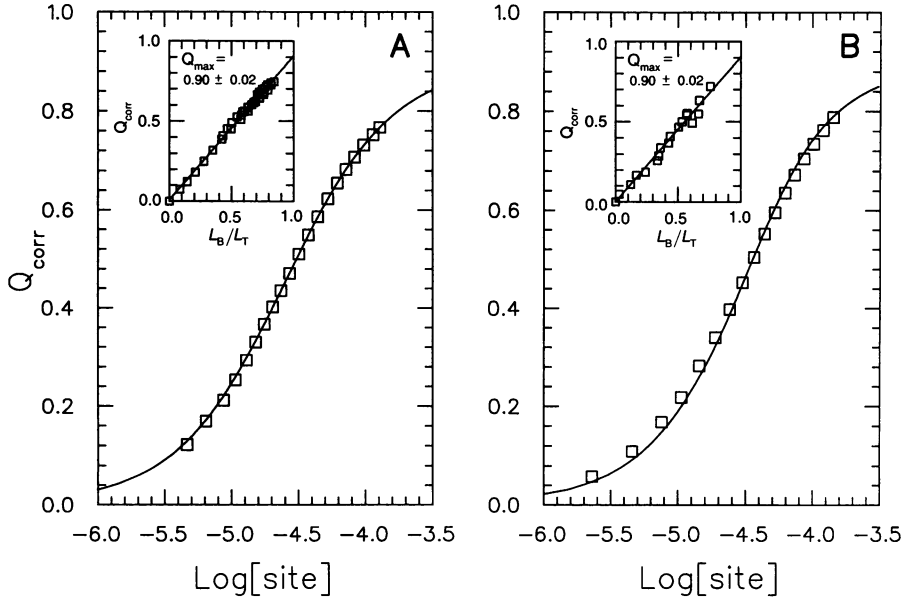

FIG. 1. Corrected tryptophan fluorescence quenching (Q_{corr}) as a function of DNA site concentration for reverse titrations of the octacation KWK_6-NH_2 with $dT(pdT)_{10}$ (*A*) and with poly(dT) (*B*). (*A*) Binding isotherm of KWK_6-NH_2 and $dT(pdT)_{10}$ at 0.1 M Na^+ at an initial ligand concentration of 2.5 μM. Smooth curve is the theoretical fitting using Eq. **2** with $n = 3$, $Q_{max} = 0.90$, and $K_{obs} = 4.6 \times 10^4\ M^{-1}$. (*Inset*) Q_{corr} as a function of $[L_B]/[L_T]$, where L_B is bound peptide and L_T is total peptide. Maximum fluorescence quenching, Q_{max}, is 0.90 ± 0.02 for $dT(pdT)_{10}$ at the salt concentration studied. (*B*) Binding isotherm of KWK_6-NH_2 with poly(dT) at 0.2 M Na^+ at an initial ligand concentration of 2.0 μM. Smooth curve is the fitting to Eq. **1** with $n = 8$, $Q_{max} = 0.90$, and $K_{obs} = 5.4 \times 10^4\ M^{-1}$. (*Inset*) Q_{corr} is plotted as a function of $[L_B]/[L_T]$. The same Q_{max} (0.90 ± 0.02) was observed for poly(dT) as for $dT(pdT)_{10}$.

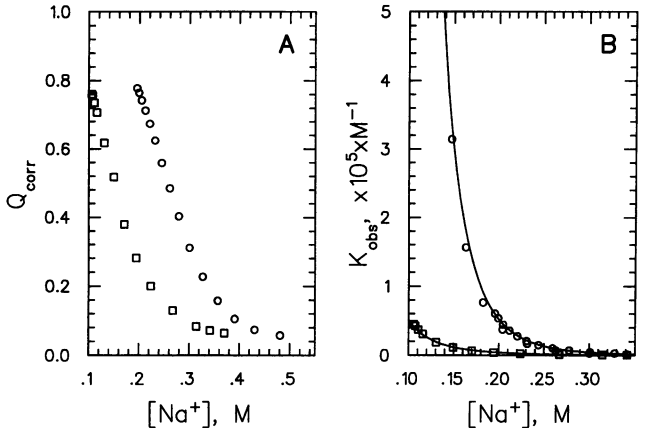

FIG. 3. Salt-back titrations of KWK_6-NH_2–DNA complexes. (*A*) Tryptophan fluorescence quenching as a function of salt concentration in a typical salt-back titration for KWK_6-NH_2 binding to poly(dT) (○) and to dT(pdT)$_{10}$ (□). (*B*) Salt concentration dependences of K_{obs} for KWK_6-NH_2 binding to poly(dT) (○) and to dT(pdT)$_{10}$ (□). Smooth curves were generated using the power functions $K_{obs} = 2.8[Na^+]^{-6.1}$ for poly(dT) and $K_{obs} = 13[Na^+]^{-3.6}$ for dT(pdT)$_{10}$.

tration. However, because K_{obs} for poly(dT) is much more strongly dependent on salt concentration than is K_{obs} for dT(pdT)$_{10}$, K_{obs} for poly(dT) becomes significantly larger than for dT(pdT)$_{10}$ below 0.3 M salt. At 0.2 M salt, K_{obs} is 5.4×10^4 M^{-1} for poly(dT) and 4.3×10^3 M^{-1} for dT(pdT)$_{10}$. At 0.1 M salt, K_{obs} for poly(dT) becomes almost 10^2 times larger ($\approx 3.5 \times 10^6$ vs. $\approx 4.6 \times 10^4$ M^{-1}) than for dT(pdT)$_{10}$!

Large Differences in S_aK_{obs} for L^{8+} Binding to Poly(dT) and to dT(pdT)$_{10}$. Fig. 4 shows $\log K_{obs}$ as a function of $\log a_\pm$ based on the salt-back titration data. The $\log K_{obs} - \log a_\pm$ plots can be well described using weighted quadratic fits. From the fits, values of S_aK_{obs} at each salt concentration are obtained by evaluating $d\log K_{obs}/d\log a_\pm$. Large differences in S_aK_{obs} for L^{8+} binding to poly(dT) and to dT(pdT)$_{10}$ at salt concentrations below 0.3 M have been observed. At 0.2 M salt ($a_\pm = 0.15$ M), S_aK_{obs} is -6.5 ± 0.2 for binding to poly(dT) and -3.5 ± 0.1 for binding to dT(pdT)$_{10}$. S_aK_{obs} changes slightly with salt concentrations, from -6.9 ± 0.1 (0.15 M salt) to -6.2 ± 0.2 (0.25 M salt) for binding to poly(dT) and from -4.1 ± 0.1 to -3.1 ± 0.1 for binding to dT(pdT)$_{10}$ over the same salt concentration range. PB calculations of S_aK_{obs} as functions of salt concentrations for binding of L^{8+} to oligomeric and

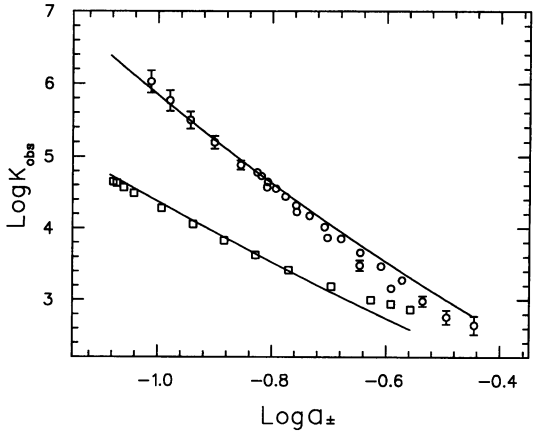

FIG. 4. Salt concentration dependences of K_{obs} for KWK_6NH_2 binding to poly(dT) (○) and to dT(pdT)$_{10}$ (□) illustrated by $\log K_{obs} - \log a_\pm$ plots. Uncertainties are SDs of means of multiple measurements. Absence of error bars implies that they are no greater than the size of the data point. Fitted curves are based on PB calculations using the standard (**b**/ε/**a**) model.

polymeric DNA, obtained over the experimental range of salt concentrations, were integrated to obtain $\log K_{obs}$ as a function of $\log a_\pm$. The integration constants to construct $\log K_{obs} - \log a_\pm$ plots were obtained from the (interpolated) experimental values of $\log K_{obs}$ at 0.2 M salt. Using the standard (**b**/ε/**a**) model (cf. *Materials and Methods*), the PB calculations shown in Fig. 4 are in very good agreement with our experimental results. Calculated values of S_aK_{obs} at 0.2 M for binding of L^{8+} to polymeric (−5.9) and oligomeric (−4.1) DNA are comparable to the corresponding experimental values (-6.5 ± 0.2 and -3.5 ± 0.1), respectively. The experimental difference between S_aK_{obs} for polymeric and oligomeric DNA is actually somewhat larger than predicted by these PB calculations. The PB calculations also predict some upward curvature of a $\log K_{obs} - \log a_\pm$ plot, as observed experimentally at sufficiently low $a_\pm$ (cf. Fig. 4).

DISCUSSION

S_aK_{obs} for L^{8+} Binding to Poly(dT) Is Dominated by Cation Release from Polymeric DNA. The thermodynamic effects of excess uniunivalent salt concentration on a binding equilibrium (S_aK_{obs}) involving oligocationic ligands are most fundamentally analyzed in terms of differences of the preferential interaction coefficients of products and reactants (cf. Eq. **3**). Each term ($|Z_J| + 2\Gamma_J$) in Eq. **3** can be interpreted as the "thermodynamic extent of association" of the univalent counterion with the indicated species (Na^+ with DNA; OAc^- with KWK_6-NH_2) (8, 22). Interpretation of our experimental results in terms of Eq. **3** indicates that S_aK_{obs} for binding of L^{8+} to polymeric DNA is dominated by the release of cations that had been thermodynamically associated with DNA. S_aK_{obs} may be resolved into two thermodynamic contributions: one from the release of anions from the ligand upon complexation [$-(|Z_L| + 2\Gamma_L)$] and the other from the release of cations from the DNA upon complexation [$(|Z_C| + 2\Gamma_C) - (|Z_D| + 2\Gamma_D)$]. Anion association with the ligand in the complex is neglected, because in this model all positive charges on the ligand are neutralized by DNA phosphates (8). As a simple approximation, contributions to $|S_aK_{obs}|$ for binding of L^{8+} to dT(pdT)$_{10}$ from cation and anion release are assumed equivalent: both ≈ 1.8 at 0.2 M salt. This approximation probably underestimates the contribution arising from cation release from the oligomeric DNA and consequently overestimates the contribution from anion release from the ligand. Our grand canonical Monte Carlo (GCMC) simulations on a related system (8) and PB calculations (data not shown) indicate that the contribution to $|S_aK_{obs}|$ from cation release from dT(pdT)$_{10}$ is somewhat larger ($\approx 10\%$) than that from anion release from L^{8+}. Clearly, this approximation does not alter our conclusions that the dominant contribution to $|S_aK_{obs}|$ for binding of L^{8+} to polymeric DNA must be from cation release (4.7 at 0.2 M salt; >70% of the total effect) while anion release from the ligand (1.8 at 0.2 M salt) contributes <30% of the effect. The extent of cation release from poly(dT) (4.7) is ≈ 2.6-fold larger than from dT(pdT)$_{10}$ (1.8) at 0.2 M salt.

Large Differences Are Observed in the Effects of Salt Concentration on Oligocation Binding to Poly- and Oligonucleotides. The large differences in K_{obs} (>10-fold) and in $|S_aK_{obs}|$ (3.0 ± 0.2) at 0.2 M NaOAc ($a_\pm = 0.15$ M) that we observe between polymeric and oligomeric DNA are direct consequences of the polyelectrolyte effect on oligocation binding to DNA. Our theoretical analyses (PB and GCMC) also have predicted large differences in salt–oligoelectrolyte and salt–polyelectrolyte interactions (this work and ref. 8). Another recent PB calculation also predicted a significant effect of oligoanion length on the salt concentration dependence of binding a spherical divalent cation to a cylindrical oligoanion (but predicted a much smaller effect on binding the dicationic drug 4′,6-diamidino-2-phenylindole to oligonucleo-

tides) at 0.1 M salt (25). However, an alternative theoretical description of oligoelectrolyte–salt interactions based on an adaptation of molecular counterion condensation theory implies that the average extent of cation accumulation per charge is similar for short oligoelectrolytes and polyelectrolytes at any excess salt concentration above 10 mM (11). The resulting thermodynamic implication is that S_aK_{obs} (as well as K_{obs}) for L^{8+} binding to poly(dT) and $dT(pdT)_{10}$ should be similar above 10 mM salt. However, we report large differences in K_{obs} (>10-fold) and in $|S_aK_{obs}|$ (3.0 ± 0.2) at 0.2 M salt (cf. Fig. 4). These large differences are qualitatively in accord with previous GCMC (8) and PB (this work and ref. 25) simulations but inconsistent with theories (11, 12) that predict essentially no difference in cation accumulation between an oligoelectrolyte and a polyelectrolyte under the conditions examined here. Our experimental results demonstrate directly the importance of polyelectrolyte effects on binding of oligocationic ligands, even at relatively high salt concentrations (≲0.3 M).

Is the Standard Model for the DNA Solution Sufficient to Account for S_aK_{obs}? According to the standard model, the fundamental structural parameters of a cylindrical DNA model are the radius of the cylinder and the average axial charge separation (8). Fine structural details have been claimed to be of primary importance, and interactions with distant charges of less importance, for understanding electrostatic contributions to oligocation–DNA and protein–DNA interactions at typical experimental salt concentrations (9, 13). However, the PB calculations of ligand binding thermodynamics presented here demonstrate the sufficiency of a small number of important averaged structural parameters (**a, b,** and, for oligomers, the number of charges) in addition to the dielectric constant of pure solvent. The ability of the standard model to predict S_aK_{obs} for oligocation binding is consistent with the inference that the magnitude of S_aK_{obs} is determined primarily by the polyelectrolyte character of the DNA. At least at salt concentrations ≲ 0.3 M, the effective range of electrostatic interactions is large enough so that local three-dimensional structural details are not needed to account for the magnitudes of S_aK_{obs} for binding of simple oligocations to short and long DNA. The small, apparently systematic deviation (outside experimental uncertainty) of the calculated curve from the data (cf. Fig. 4) may be attributable to specific effects of ions or water (hydration) not described by any purely electrostatic calculation of S_aK_{obs} (4, 26) or may reflect some inaccuracy of structural parameters (**a** and **b**), which were not optimized. A recent review (14) considers the related (currently unresolved) question of how much structural detail is required at typical salt concentrations to predict or analyze the electrostatic component of protein–DNA binding thermodynamics.

Implications for Protein–Nucleic Acid Interactions. A recent PB-based study (10) and its extension (25), which used detailed structural models to analyze several site-specific protein–DNA interactions, concluded that the contribution to S_aK_{obs} from salt interactions (i.e., nonspecific ion interactions) with the protein is substantial. These PB calculations included only purely nonspecific electrostatic interactions and thus did not attempt to introduce any effect resulting from binding of particular types of ions to specific sites on the protein. Although large contributions to S_aK_{obs} from the protein are observed experimentally in some protein–DNA systems, these appear to be due to specific binding of ions (in particular anions) to the protein (27). No experimental indication exists that purely coulombic nonspecific interactions of salt ions with proteins make a major contribution to S_aK_{obs}. Indeed, the results reported here demonstrate a profound asymmetry between the thermodynamic contributions to S_aK_{obs} from a polymeric DNA and an oligocationic ligand (cf. Eq. **3**). Most of the large salt concentration effect on the binding is due to nonspecific salt–DNA interactions rather than either specific or nonspecific salt–ligand interactions. This finding is consistent with previous results demonstrating that S_aK_{obs} for binding of oligolysine peptides to DNA is independent of the nature of the monovalent cation and anion (6). A large asymmetry in thermodynamic contributions to S_aK_{obs} may also be expected for protein–nucleic acid interactions where the DNA is a polyanion if the binding site on the protein ligand behaves locally as an oligocation, and if specific ion–protein and specific ion–DNA interactions (i.e., site binding) are absent (28).

CONCLUSIONS

At salt concentrations in the typical experimental range (0.1–0.3 M), the experimental and theoretical results presented here demonstrate important thermodynamic consequences of the long-range nonspecific electrostatic interactions of salt ions with polyions having a high average axial charge density. Our PB calculations show that the primary origin of the large effect of salt concentration on the binding of an oligocation to polymeric DNA is the release of thermodynamically associated cations from the nucleic acid rather than of anions from the ligand. Hence, to describe this phenomenon the appellation "polyelectrolyte effect" is appropriate. We also demonstrate that at typical experimental conditions key preaveraged structural parameters (**a** and **b**) of the nucleic acid capture the essence of the polyelectrolyte effect and that atomic detail is not a prerequisite to account for the salt concentration effects observed here.

Systematic studies of the approach of K_{obs} and S_aK_{obs} to their polyelectrolyte limits as functions of salt and oligonucleotide length are in progress. The resulting data and calculations will enable a more precise determination of the effective range of electrostatic interactions in nucleic acid solutions by establishing upper bounds on the range of salt concentrations over which differences in ligand binding energetics can be discerned between polymeric DNA and oligonucleotides of varying lengths. At high enough salt concentrations the effective range of electrostatic interactions must be reduced to the extent that short-range (noncovalent) interactions between salt ions and the surface of a nucleic acid, as well as interactions involving water molecules, become significant. Under these conditions the inclusion in a theoretical model of fine structural details for each participant in a nucleic acid binding equilibrium is likely to be necessary, but not sufficient, to construct a rigorous theoretical description of the binding thermodynamics.

We thank M. Capp for helping with the purification of the oligopeptide and the oligonucleotide, Dr. S. Padmanabhan for helping with the oligopeptide synthesis, and Prof. L. Smith and Dr. M. Fitzgerald for mass spectrometric identification of the oligopeptide. This work was supported by National Institutes of Health Grants GM34351 (M.T.R.) and GM30498 (T.M.L.).

1. Kowalczykowski, S. C., Lonberg, N., Newport, J. W. & von Hippel, P. H. (1981) *J. Mol. Biol.* **145,** 75–104.
2. Lohman, T. M. & Ferrari, M. E. (1994) *Annu. Rev. Biochem.* **63,** 527–570.
3. Record, M. T., Jr., Lohman, T. M. & de Haseth, P. (1976) *J. Mol. Biol.* **107,** 145–158.
4. Record, M. T., Jr., Anderson, C. F. & Lohman, T. M. (1978) *Q. Rev. Biophys.* **11,** 103–178.
5. Latt, S. A. & Sober, H. A. (1967) *Biochemistry* **6,** 3307–3314.
6. Mascotti, D. P. & Lohman, T. M. (1990) *Proc. Natl. Acad. Sci. USA* **87,** 3142–3146.
7. Mascotti, D. P. & Lohman, T. M. (1993) *Biochemistry* **32,** 10568–10579.
8. Olmsted, M. C., Bond, J. P., Anderson, C. F. & Record, M. T., Jr. (1995) *Biophys. J.* **68,** 634–647.
9. Misra, V. K., Hecht, J. L., Sharp, K. A., Friedman, R. A. & Honig, B. (1994) *J. Mol. Biol.* **238,** 264–280.

10. Misra, V. K., Sharp, K. A., Friedman, R. A. & Honig, B. (1994) *J. Mol. Biol.* **238,** 245–263.
11. Fenley, M. O., Manning, G. S. & Olson, W. K. (1990) *Biopolymers* **30,** 1191–1203.
12. Dewey, T. G. (1990) *Biopolymers* **29,** 1793–1799.
13. Honig, B. & Nicholls, A. (1995) *Science* **268,** 1144–1149.
14. Anderson, C. F. & Record, M. T., Jr. (1995) *Annu. Rev. Phys. Chem.* **46,** 657–700.
15. Fasman, G. D. (1975) *CRC Handbook of Biochemistry and Molecular Biology* (CRC, Boca Raton, FL), 3rd Ed., p. 589.
16. Houghten, R. A., Degraw, S. T., Bray, M. K., Hoffman, S. R. & Frizell, N. D. (1986) *BioTechniques* **4,** 522–528.
17. Edelhoch, H. (1967) *Biochemistry* **6,** 1948–1954.
18. Lohman, T. M. & Mascotti, D. P. (1992) *Methods Enzymol.* **212,** 424–458.
19. Bujalowski, W. & Lohman, T. M. (1987) *Biochemistry* **26,** 3099–3106.
20. McGhee, J. D. & von Hippel, P. H. (1974) *J. Mol. Biol.* **86,** 469–489.
21. Weast, R. C. (1978) *CRC Handbook of Chemistry and Physics* (CRC, Boca Raton, FL), 59th Ed., p. D-205.
22. Anderson, C. F. & Record, M. T., Jr. (1993) *J. Phys. Chem.* **97,** 7116–7126.
23. Allison, S. A. (1994) *J. Phys. Chem.* **98,** 12091–12096.
24. Olmsted, M. C., Anderson, C. F. & Record, M. T., Jr. (1991) *Biopolymers* **31,** 1593–1604.
25. Sharp, K. A., Friedman, R. A., Misra, V., Hecht, J. & Honig, B. (1995) *Biopolymers* **36,** 245–262.
26. Record, M. T., Jr., & Anderson, C. F. (1995) *Biophys. J.* **68,** 786–794.
27. Overman, L. B. & Lohman, T. M. (1994) *J. Mol. Biol.* **236,** 165–178.
28. Capp, M. W., Cayley, D. S., Zhang, W., Guttman, H. J., Melcher, S., Spolar, R. S., Anderson, C. F. & Record, M. T., Jr. (1996) *J. Mol. Biol.*, in press.